Sudakov suppression and the proton form factor

Hsiang-nan Li
Institute of Physics, Academia Sinica, Taipei, Taiwan 11529, Republic of China
and Institute for Theoretical Physics, State University of New York, Stony Brook, New York 11794-3840
(Received 13 April 1993)

The proton Dirac form factor is calculated using the modified factorization formula proposed by Li and Sterman, which takes into account Sudakov suppression of elastic scattering for soft gluon exchange. The results for $\Lambda_{\rm QCD}=0.1-0.2$ GeV are in good agreement with experimental data above the energy scale of 3 GeV. The calculation involves no phenomenological parameters such as a gluon mass and the conclusions are insensitive to different models of wave functions.

PACS number(s): 13.40.Fn, 12.38.Bx, 14.20.Dh

I. INTRODUCTION

The nucleon electromagnetic form factors have been widely calculated to leading power in perturbative QCD (PQCD) [2–10]. The main approach is based on the factorization theorem, in which the asymptotic expression for the nucleon magnetic form factor

$$G_M(Q^2)=F_1(Q^2)+F_2(Q^2)$$

is written as the convolution of a hard-scattering kernel T_H and nucleon distribution amplitudes ϕ. Since $F_2(Q^2)=O(1/Q^6)$ is much smaller than $F_1(Q^2)=O(1/Q^4)$ in the asymptotic region [7], we concentrate on the proton Dirac form factor F_1^p, as illustrated in Fig. 1:

$$F_1^p(Q^2)=\int_0^1 (dx)(dx')\phi^*(x_i',\mu^2)T_H(x_i,x_i',Q^2,\mu^2)\times\phi(x_i,\mu^2)\ , \tag{1}$$

where μ is the renormalization and factorization scale, $Q^2=2P\cdot P'$, and

$$(dx)=dx_1dx_2dx_3\delta\left[\sum_{i=1}^{3}x_i-1\right]\ .$$

x_i is the momentum fraction of the valence quark i in the parton model, in which all the lines are thought of as near or on the mass shell. T_H contains only lines that are far off shell. Variables with and without a prime denote the initial and final states, respectively.

The above perturbative calculation at currently accessible Q^2 has been criticized [6,11]. A modified factorization formula for the pion electromagnetic form factor with Sudakov effects included has been proposed, which enlarges the applicability of PQCD down to the regime of several GeV^2. In this paper we will extend this approach to the proton Dirac form factor, and show that the modified formalism gives reliable predictions which are in good agreement with experimental data.

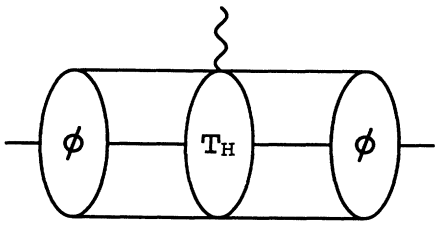

FIG. 1. The basic diagram for the proton Dirac form factor.

Before presenting out derivation, we review why the applicability of PQCD to such processes is a subject of controversy. It has been shown that the asymptotic proton wave function $\phi(x_i,\mu^2)\propto x_1x_2x_3$ fails to give the correct sign for F_1^p and generates much smaller values than data [3,10]. Highly asymmetric distribution amplitudes [7,12,13] based on QCD sum rules reverse the sign and enlarge the magnitude of predictions derived from Eq. (1). Careful analysis reveals that the enlargement is due to amplification of the contributions from the end-point region of x [6,11]. T_H for the proton form factor is proportional to the product of two hard gluon propagators,

$$\alpha_s^2(\mu^2)/[x_ix_i'Q^2(1-x_j)(1-x_j')Q^2]\ ,$$

to the lowest order as shown in Fig. 2. Higher-order corrections in T_H then produce logarithms such as $\ln(x_ix_i'Q^2)$ and

$$\ln[(1-x_j)(1-x_j')Q^2]\ .$$

To eliminate the logarithms, the natural choices for μ^2 are $x_ix_i'Q^2$ and $(1-x_j)(1-x_j')Q^2$ for each gluon. These choices can give closer results to data [8], but in the dominant end-point region, the running coupling constants $\alpha_s(x_ix_i'Q^2)$ or

$$\alpha_s[(1-x_j)(1-x_j')Q^2]$$

diverge. The self-consistency of perturbative calculation is thus in danger.

A modification to avoid the divergences has been proposed by introducing a cutoff in the formula for α_s [8,14]:

$$\alpha_s(Q^2)=\frac{4\pi}{\beta\ln[(Q^2+4m_g^2)/\Lambda^2]}\ , \tag{2}$$

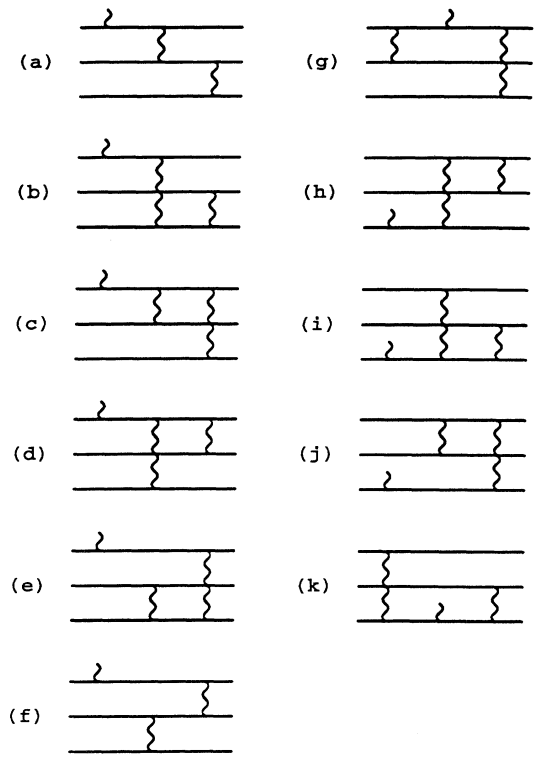

FIG. 2. Independent lowest-order diagrams for the evaluation of the proton Dirac form factor. The bottom line represents the d quark, corresponding to x_3 (x_3') for the incoming (outgoing) proton.

where $\Lambda \equiv \Lambda_{\rm QCD}$ is the QCD scale parameter, and $\beta = 11 - 2n_f/3$ for n_f quark flavors. m_g is interpreted as a dynamical gluon mass which is acquired from the low-momentum region of radiative corrections that induce the Q^2 dependence of α_s. The leading-order PQCD predictions are then stabilized at low-momentum transfers. The value of m_g has to be determined by matching the predictions with data. However, the results from Eq. (1) are sensitive to the variation of m_g around the best choice $m_g^2 \approx 0.3$ GeV^2 [8]. The theory with this form of cutoff then becomes less predictive.

In deriving Eq. (1), one neglects transverse momenta $\mathbf{k}_T$ that flow into the hard-scattering subprocess with valence quarks because contributions due to $\mathbf{k}_T$ are always suppressed by powers of Q^2 for x not close to 0 and 1. The end-point difficulties encountered in the standard formula indicate that these higher-power effects are crucial to the analysis of the process. Hence, we kept $\mathbf{k}_T$ at the outset in the derivation of the new perturbative expression for the pion form factor proposed in Ref. [1]. We analyzed the amplitude in the Fourier transform space of $\mathbf{k}_T$, denoted by b, the transverse separation between valence quarks. The quantity $1/b^2$, now considered as one of the characteristic mass scales of the hard scattering, should be substituted for the argument of α_s if $1/b^2 > xx'Q^2$. The soft region is then characterized by large b and small x.

Furthermore, we find that the resummation of radiative corrections behaves as

$$\exp[-\text{const} \times \ln(Q) \ln(\ln Q/\ln b)]$$

in the leading logarithmic approximation, which suppresses the elastic scattering at large spatial separation. This property, the Sudakov suppression [15,16], makes the nonperturbative contributions from large b, no matter what x is, less important, without introducing any phenomenological parameters other than Λ. The suppression of the end-point contribution by Sudakov effects has been pointed out by Lepage and Brodsky [2]. Note that the new perturbative expression will reduce to the standard one in Eq. (1) as $Q \to \infty$ but, at lower momentum transfers, its extra b (or $\mathbf{k}_T$) dependence makes the perturbative theory more self-consistent.

We concentrate only on the $\mathbf{k}_T$ effects in this paper, excluding the contributions from extra partons that enter T_H, which are also of higher twist. We will apply the new expression to the proton Dirac form factor, with the use of the Chernyak-Zhitnitsky (CZ) [7], King-Sachrajda (KS) [12] wave functions. The dependence of $Q^4 F_1^p(Q^2)$ on a cutoff in b, instead of in x [11,17], is studied in order to investigate the importance of the perturbative region. It is found that the inclusion of Sudakov suppression produces results that are numerically similar to the standard approaches [7–9]. Moreover, our results are reliable in the sense that the perturbative contribution dominates, and are consistent with experimental data [18].

The modified factorization formula for the proton Dirac form factor is derived in Sec. II. In Sec. III, the explicit b dependence of the distribution amplitude and the complete expression of Sudakov logarithms are exhibited. In Sec. IV, we insert the CZ and KS wave functions to obtain numerical answers and analyze how the contributions are distributed in b space. The results are also compared with the data. We summarize our ideas in Sec. V.

II. FACTORIZATION

The standard factorization procedures for QCD processes require investigation of leading regions of momentum space in radiative corrections, where dominant contributions arise. The leading regions depend on the gauge. For the present work, it is simplest to choose a physical gauge, such as the axial gauge, with the gauge-fixing parameter n^μ a linear combination of dimensionless vectors v^μ and v'^μ, which are lightlike and in the directions of the external protons. Our approach to factorization follows a similar reasoning to that which leads to Eq. (1) [19–21], but without the assumption $xx'Q^2 \gg \mathbf{k}_T^2$. The basic analysis of factorization for exclusive processes has been given in Ref. [22].

There are two types of radiative corrections to the basic scattering process of Fig. 1. For two-particle reducible diagrams such as Figs. 3(a) and 3(b), both the collinear region, with an extra gluon parallel to either the incoming or outgoing proton, and the soft region, with the gluon's momentum much smaller than Q^2, are important on a diagram-by-diagram basis. The soft divergences will

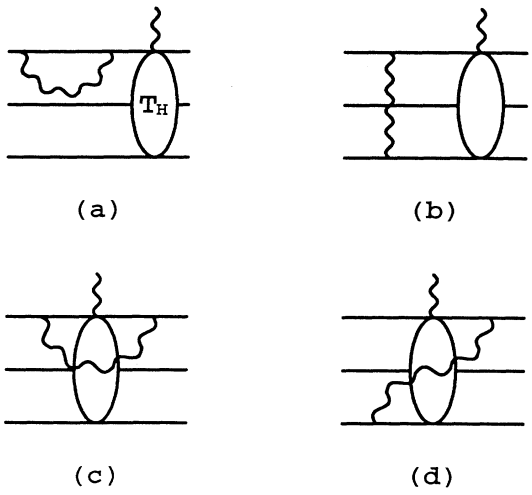

FIG. 3. Radiative corrections to the basic scattering diagram.

cancel between these diagrams, at least when all lines in T_H are far off shell. Their combination then produces a single collinear logarithm which can be grouped into the distribution amplitudes. In fact, these are the very radiative corrections that generate Sudakov suppression when lines in T_H approach the mass shell and the cancellation mentioned above fails. The two-particle irreducible diagrams Figs. 3(c) and 3(d) contain only soft divergences, which cancel similarly. Once the soft divergences are removed, these types of corrections are dominated by momenta of order Q^2 and their contributions can be absorbed into the hard part. Such cancellation applies to all orders in perturbative theory. Based on the above reasoning, the factorization formula for the proton Dirac form factor includes only three factors [1]

$$F_1^p(Q^2)=\int_0^1 (dx)(dx')(d\mathbf{k}_T)(d\mathbf{k}'_T)\bar{Y}_{\alpha'\beta'\gamma'}(k'_i,P',\mu) \times H_{\alpha'\beta'\gamma'\alpha\beta\gamma}(k_i,k'_i,Q,\mu)Y_{\alpha\beta\gamma}(k_i,P,\mu) , \tag{3}$$

where

$$(d\mathbf{k}_T)=d\mathbf{k}_{T_1}d\mathbf{k}_{T_2}d\mathbf{k}_{T_3}\delta\left[\sum_{i=1}^{3}\mathbf{k}_{T_i}\right]$$

and the scale μ is introduced by necessary renormalizations. The initial distribution amplitude $Y_{\alpha\beta\gamma}(k_i,P,\mu)$, containing the nonperturbative dynamics of the proton, is defined by the matrix element of three local operators in the axial gauge [7,15]:

$$\begin{aligned} Y_{\alpha\beta\gamma}&=\frac{1}{2\sqrt{2}N_c}\int\prod_{l=1}^{2}\frac{dy_l^- d\mathbf{y}_l}{(2\pi)^3}e^{ik_l\cdot y_l}\epsilon^{abc}\langle 0|T[u_\alpha^a(y_1)u_\beta^b(y_2)d_\gamma^c(0)]|P\rangle \\ &=\frac{f_N(\mu)}{8\sqrt{2}N_c}[(\not{P}C)_{\alpha\beta}(\gamma_5 N)_\gamma V(k_i,P,\mu)+(\not{P}\gamma_5 C)_{\alpha\beta}N_\gamma A(k_i,P,\mu)-(\sigma_{\mu\nu}P^\nu C)_{\alpha\beta}(\gamma^\mu\gamma_5 N)_\gamma T(k_i,P,\mu)] , \end{aligned} \tag{4}$$

where $|P\rangle$ is the incoming proton state with momentum $P=(Q/\sqrt{2},0,0)$, u and d are quark fields, a, b, and c are color indices, and α, β, and γ are spinor indices. The loop momentum k_i, with the longitudinal component $k_i^+=x_iP^+$ and transverse component $\mathbf{k}_{T_i}$, is carried by the valence quark i. In our notation, 1 and 2 label the two u quarks and 3 labels the d quark. The second form with the explicit Dirac matrix structure shown [7] is obtained from the spin property of quark fields, where $N_c=3$ is the color number, N is the proton spinor, C is the charge conjugation matrix, and $\sigma_{\mu\nu}\equiv[\gamma_\mu,\gamma_\nu]/2$. The dimensional constant f_N, analogous to the pion decay constant f_π, is determined by the normalization condition of the distribution amplitude [23]. $\bar{Y}_{\alpha'\beta'\gamma'}(k'_i,P',\mu)$ is defined similarly for the final state with $P'=(0,Q/\sqrt{2},0)$ and $k_i'^-=x_i'P'^-$.

From the permutation symmetry between the two u quarks, one obtains the relations [7]

$$\begin{aligned} &V(k_1,k_2,k_3,P,\mu)=V(k_2,k_1,k_3,P,\mu) , \\ &A(k_1,k_2,k_3,P,\mu)=-A(k_2,k_1,k_3,P,\mu) , \\ &T(k_1,k_2,k_3,P,\mu)=T(k_2,k_1,k_3,P,\mu) . \end{aligned} \tag{5}$$

The requirement that the total isospin of the three quarks be equal to $\frac{1}{2}$ leads to the further relations among the functions V, A, and T [7]:

$$2T(k_1,k_2,k_3,P,\mu)=\psi(k_1,k_3,k_2,P,\mu)+\psi(k_2,k_3,k_1,P,\mu) , \tag{6}$$

where

$$\psi(k_1,k_2,k_3,P,\mu)=V(k_1,k_2,k_3,P,\mu)-A(k_1,k_2,k_3,P,\mu) . \tag{7}$$

Combining Eqs. (5) and (6), we have

$$\begin{aligned} V(k_1,k_2,k_3,P,\mu)&=\tfrac{1}{2}[\psi(k_2,k_1,k_3,P,\mu)+\psi(k_1,k_2,k_3,P,\mu)] , \\ A(k_1,k_2,k_3,P,\mu)&=\tfrac{1}{2}[\psi(k_2,k_1,k_3,P,\mu)-\psi(k_1,k_2,k_3,P,\mu)] . \end{aligned} \tag{8}$$

Hence, the analysis in fact involves only one independent wave function ψ.

The hard-scattering kernel

$$H_{\alpha'\beta'\gamma'\alpha\beta\gamma}(k_i,k'_i,Q,\mu)$$

can be calculated perturbatively in terms of the diagrams in Fig. 2. To the lowest order of α_s with two hard exchanged gluons, 42 diagrams can be drawn for the proton

Dirac form factor. This number is reduced to 21 when the permutation symmetry between the incoming and outgoing protons is considered. Those 21 diagrams are further divided into two categories which can be transformed into each other by interchanging the two u quarks, so that it is enough to calculate only 11 of them, as shown in Fig. 2. The diagrams with three-gluon vertices vanish at leading twist and are thus neglected. A typical calculation of the integrand

$$\bar{Y}_{\alpha'\beta'\gamma} H_{\alpha'\beta'\gamma'\alpha\beta\gamma} Y_{\alpha\beta\gamma}$$

for one of these diagrams, using the property of the Dirac and charge conjugation matrices, is presented in Appendix A in detail. Here, we just display the results in Table I. The index of the wave function ψ denotes the sequence of the arguments k_i. Note that the formulas in Table I are derived through the approximation that the transverse momenta carried by the virtual quarks in the hard-scattering subdiagram are neglected [1] since, compared to the virtual gluons, they give linear, rather than quadratic, divergences in x. This approximation, as explained in Appendix A, equates the initial and final transverse distances between all pairs of valence quarks. The complexity of the analysis is then reduced and numerical evaluation becomes possible. At the same time, fermion energies such as $x_i Q^2$ will not be among the characteristic scales of the hard scattering, and the evolution of H in Q is simpler. The accuracy of this approximation will be discussed in Appendix B.

Applying a series of variable changes as shown in Table I, the summation of the contributions over the 42 diagrams in Eq. (3), can be carried out easily. For instance, we observe that the formula (a), if the variables with indices 2 and 3 are interchanged, will be the same as (b) except for the sequence of the arguments in the wave functions. Repeating such variable changes on every formula in Table I, all the contributions to $F_1^p(Q^2)$ can be summed into only two terms

TABLE I. The expressions of the integrand $\bar{Y}_{\alpha'\beta'\gamma'} H_{\alpha'\beta'\gamma'\alpha\beta\gamma} Y_{\alpha\beta\gamma}$ for the diagrams in Fig. 2. ψ_{123} is the brief symbol for $\psi(k_1,k_2,k_3,P,\mu)$ and ψ'_{123} for $\psi(k'_1,k'_2,k'_3,P',\mu)$. For each diagram, (a)–(k), row (1) is the original expression. Row (2) is the necessary series of variable changes to bring row (1) into the desired form. Row (3) is the expression after variable changes. The detailed derivations refer to Appendix A.

Diagram	$\bar{Y}HY/(4\pi^2\alpha_s^2 f_N^2/27)$
(a) (1)	$\dfrac{e_u(\psi_{123}\psi'_{123}+4T_{123}T'_{123})}{(1-x_1)(1-x'_1)[(1-x_1)(1-x'_1)Q^2+(\mathbf{k}_{T_1}-\mathbf{k}'_{T_1})^2][x_3x'_3Q^2+(\mathbf{k}_{T_3}-\mathbf{k}'_{T_3})^2]}$
(2)	$2\leftrightarrow 3$
(3)	$\dfrac{e_u(\psi_{132}\psi'_{132}+4T_{132}T'_{132})}{(1-x_1)(1-x'_1)[(1-x_1)(1-x'_1)Q^2+(\mathbf{k}_{T_1}-\mathbf{k}'_{T_1})^2][x_2x'_2Q^2+(\mathbf{k}_{T_2}-\mathbf{k}'_{T_2})^2]}$
(b) (1)	$\dfrac{e_u(\psi_{123}\psi'_{123}+4T_{123}T'_{123})}{(1-x_1)(1-x'_1)[(1-x_1)(1-x'_1)Q^2+(\mathbf{k}_{T_1}-\mathbf{k}'_{T_1})^2][x_2x'_2Q^2+(\mathbf{k}_{T_2}-\mathbf{k}'_{T_2})^2]}$
(2)	None
(3)	$\dfrac{e_u(\psi_{123}\psi'_{123}+4T_{123}T'_{123})}{(1-x_1)(1-x'_1)[(1-x_1)(1-x'_1)Q^2+(\mathbf{k}_{T_1}-\mathbf{k}'_{T_1})^2][x_2x'_2Q^2+(\mathbf{k}_{T_2}-\mathbf{k}'_{T_2})^2]}$
(c) (1)	$-\dfrac{e_u 4T_{123}T'_{123}}{(1-x_1)(1-x'_2)[x_2x'_2Q^2+(\mathbf{k}_{T_2}-\mathbf{k}'_{T_2})^2][x_3x'_3Q^2+(\mathbf{k}_{T_3}-\mathbf{k}'_{T_3})^2]}$
(2)	$1\rightarrow 3,2\rightarrow 1,3\rightarrow 2$
(3)	$-\dfrac{e_u 4T_{312}T'_{312}}{(1-x_3)(1-x'_1)[x_1x'_1Q^2+(\mathbf{k}_{T_1}-\mathbf{k}'_{T_1})^2][x_2x'_2Q^2+(\mathbf{k}_{T_2}-\mathbf{k}'_{T_2})^2]}$
(d) (1)	$-\dfrac{e_u\psi_{123}\psi'_{123}}{(1-x_1)(1-x'_3)[x_2x'_2Q^2+(\mathbf{k}_{T_2}-\mathbf{k}'_{T_2})^2][x_3x'_3Q^2+(\mathbf{k}_{T_3}-\mathbf{k}'_{T_3})^2]}$
(2)	$1\leftrightarrow 3$
(3)	$-\dfrac{e_u\psi_{321}\psi'_{321}}{(1-x_3)(1-x'_1)[x_1x'_1Q^2+(\mathbf{k}_{T_1}-\mathbf{k}'_{T_1})^2][x_2x'_2Q^2+(\mathbf{k}_{T_2}-\mathbf{k}'_{T_2})^2]}$
(e)	0
(f)	0

TABLE I. (*Continued*).

Diagram	$\bar{Y}HY/(4\pi^2\alpha_s^2 f_N^2/27)$
(g) (1)	$\dfrac{e_u\psi_{213}\psi'_{213}}{(1-x_3)(1-x'_2)[x_2x'_2Q^2+(\mathbf{k}_{T_2}-\mathbf{k}'_{T_2})^2][x_3x'_3Q^2+(\mathbf{k}_{T_3}-\mathbf{k}'_{T_3})^2]}$
(2)	$1\leftrightarrow 3,\quad x_i\leftrightarrow x'_i$
(3)	$\dfrac{e_u\psi_{231}\psi'_{231}}{(1-x_2)(1-x'_1)[x_1x'_1Q^2+(\mathbf{k}_{T_1}-\mathbf{k}'_{T_1})^2][x_2x'_2Q^2+(\mathbf{k}_{T_2}-\mathbf{k}'_{T_2})^2]}$
(h) (1)	$\dfrac{e_d(\psi_{123}\psi'_{123}+\psi_{213}\psi'_{213})}{(1-x_3)(1-x'_3)[x_2x'_2Q^2+(\mathbf{k}_{T_2}-\mathbf{k}'_{T_2})^2][(1-x_3)(1-x'_3)Q^2+(\mathbf{k}_{T_3}-\mathbf{k}'_{T_3})^2]}$
(2)	$1\leftrightarrow 3$
(3)	$\dfrac{e_d(\psi_{321}\psi'_{321}+\psi_{231}\psi'_{231})}{(1-x_1)(1-x'_1)[(1-x_1)(1-x'_1)Q^2+(\mathbf{k}_{T_1}-\mathbf{k}'_{T_1})^2][x_2x'_2Q^2+(\mathbf{k}_{T_2}-\mathbf{k}'_{T_2})^2]}$
(i) (1)	$-\dfrac{e_d\psi_{123}\psi'_{123}}{(1-x_3)(1-x'_1)[x_1x'_1Q^2+(\mathbf{k}_{T_1}-\mathbf{k}'_{T_1})^2][x_2x'_2Q^2+(\mathbf{k}_{T_2}-\mathbf{k}'_{T_2})^2]}$
(2)	None
(3)	$-\dfrac{e_d\psi_{123}\psi'_{123}}{(1-x_3)(1-x'_1)[x_1x'_1Q^2+(\mathbf{k}_{T_1}-\mathbf{k}'_{T_1})^2][x_2x'_2Q^2+(\mathbf{k}_{T_2}-\mathbf{k}'_{T_2})^2]}$
(j)	0
(k) (1)	$\dfrac{e_d 4T_{123}T'_{123}}{(1-x_2)(1-x'_1)[x_1x'_1Q^2+(\mathbf{k}_{T_1}-\mathbf{k}'_{T_1})^2][x_2x'_2Q^2+(\mathbf{k}_{T_2}-\mathbf{k}'_{T_2})^2]}$
(2)	None
(3)	$\dfrac{e_d 4T_{123}T'_{123}}{(1-x_2)(1-x'_1)[x_1x'_1Q^2+(\mathbf{k}_{T_1}-\mathbf{k}'_{T_1})^2][x_2x'_2Q^2+(\mathbf{k}_{T_2}-\mathbf{k}'_{T_2})^2]}$

$$F_1^p(Q^2)=\frac{8\pi^2}{27}\int_0^1(dx)(dx')(d\mathbf{k}_T)(d\mathbf{k}'_T)[f_N(\mu)]^2\sum_{j=1}^{2}H_j(k_i,k'_i,Q,\mu)\Psi_j(k_i,k'_i,P,P',\mu)\ . \tag{9}$$

Here we define

$$H_1=\frac{2\alpha_s^2(\mu^2)}{3[(1-x_1)(1-x'_1)Q^2+(\mathbf{k}_{T_1}-\mathbf{k}'_{T_1})^2][x_2x'_2Q^2+(\mathbf{k}_{T_2}-\mathbf{k}'_{T_2})^2]}\ ,$$
$$H_2=\frac{2\alpha_s^2(\mu^2)}{3[x_1x'_1Q^2+(\mathbf{k}_{T_1}-\mathbf{k}'_{T_1})^2][x_2x'_2Q^2+(\mathbf{k}_{T_2}-\mathbf{k}'_{T_2})^2]} \tag{10}$$

and

$$\Psi_1=\frac{2(\psi\psi')_{123}+8(TT')_{123}+2(\psi\psi')_{132}+8(TT')_{132}-(\psi\psi')_{321}-(\psi\psi')_{231}}{(1-x_1)(1-x'_1)}\ ,$$
$$\Psi_2=\frac{2(\psi\psi')_{132}-2(TT')_{123}}{(1-x_2)(1-x'_1)}+\frac{(\psi\psi')_{123}-8(TT')_{132}-2(\psi\psi')_{321}}{(1-x_3)(1-x'_1)}\ , \tag{11}$$

which group together the products of the initial and final wave functions in the notation

$$(\psi\psi')_{123}\equiv\psi(k_1,k_2,k_3,P,\mu)\psi(k'_1,k'_2,k'_3,P',\mu)\ .$$

The values of electric charge e_u and e_d have been inserted. Note that the propagator proportional to

$$1/[xx'Q^2+(\mathbf{k}_T-\mathbf{k}'_T)^2]$$

in Eq. (10) can be thought of as an approximate form to the exact one $1/(k-k')^2$ with k^- and k'^+ neglected, which is correct to the power $\mathbf{k}_T^2/Q^2$. These expressions for the hard scattering differ from those given in previous works by including transverse momentum effects, which are not negligible in the end-point region.

III. SUDAKOV SUPPRESSION

As mentioned in the Introduction, we now reexpress Eq. (9) in the Fourier transform space

$$F_1^p(Q^2)=\sum_{j=1}^{2}\frac{8\pi^2}{27}\int_0^1(dx)(dx')(d\mathbf{b})(d\mathbf{b}')[f_N(\mu)]^2H_j(x_i,x_i',\mathbf{b}_i,\mathbf{b}_i',Q,\mu)\Psi_j(x_i,x_i',\mathbf{b}_i,\mathbf{b}_i',P,P',\mu)$$
$$=\sum_{j=1}^{2}\frac{8\pi^2}{27}\int_0^1(dx)(dx')(d\mathbf{b})[f_N(\mu)]^2H_j(x_i,x_i',\mathbf{b}_i,Q,\mu)\Psi_j(x_i,x_i',\mathbf{b}_i,P,P',\mu)\ , \tag{12}$$

where $\mathbf{b}_i$ is the conjugate vector to $\mathbf{k}_{T_i}$, and

$$(d\mathbf{b})=d\mathbf{b}_1d\mathbf{b}_2/(2\pi)^4\ .$$

In the second equation, we have performed the $\mathbf{b}'$ integrations using the fact that H_j's depend only on the differences of the initial and final transverse momenta.

The leading behavior of the transformed wave function $\mathcal{P}(x_i,\mathbf{b}_i,P,\mu)$ in b has been explored in Ref. [15], where radiative corrections of the type in Figs. 3(a) and 3(b) were analyzed and resumed according to renormalization-group methods. The results are given in the form of an exponential suppression that is found to suppress the distribution amplitude at large b:

$$\mathcal{P}(x_i,\mathbf{b}_i,P,\mu)=\int(d\mathbf{k}_T)\exp\left[i\sum_{l=1}^{2}\mathbf{k}_{T_l}\cdot\mathbf{b}_l\right]\psi(k_i,P,\mu)$$
$$=\exp\left[-\sum_{l=1}^{3}\left[s(x_l,\tilde{b}_l,Q)+\int_{1/\tilde{b}_l}^{\mu}\frac{d\bar{\mu}}{\bar{\mu}}\gamma_q[g(\bar{\mu}^2)]\right]\right]\phi(x_i,w)+O(\alpha_s(w^2))\ , \tag{13}$$

where $\tilde{b}_1=|\mathbf{b}_1|$ is the distance between the first and third quarks since $\mathbf{b}_3=0$ as defined in Eq. (4), $\tilde{b}_2=|\mathbf{b}_2|$ and $\tilde{b}_3=|\mathbf{b}_1-\mathbf{b}_2|$ are defined similarly. $\gamma_q(g)=-\alpha_s/\pi$ is the anomalous dimension in axial gauge. The wave function ϕ, obtained by factoring the Q and b dependences from $\mathcal{P}$ into the exponent, coincides with the standard one in Eq. (1). $w=\min_i(1/\tilde{b}_i)$ is the evolution parameter. The Sudakov exponent $s(\xi,\tilde{b},Q)$, with $\xi=x_1$, x_2, or x_3, are expressed below in terms of

$$\hat{q}\equiv\ln[\xi Q/(\sqrt{2}\Lambda)]\ ,$$
$$\hat{b}\equiv\ln(\tilde{b}\Lambda)\ .$$

Then s, to the leading and next to leading logarithms, is given by [15]

$$s(\xi,\tilde{b},Q)=\frac{A^{(1)}}{2\beta_1}\hat{q}\ln\left[\frac{\hat{q}}{-\hat{b}}\right]+\frac{A^{(2)}}{4\beta_1^2}\left[\frac{\hat{q}}{-\hat{b}}-1\right]-\frac{A^{(1)}}{2\beta_1}(\hat{q}+\hat{b})-\frac{A^{(1)}\beta_2}{16\beta_1^3}\hat{q}\left[\frac{\ln(-2\hat{b})+1}{-\hat{b}}-\frac{\ln(2\hat{q})+1}{\hat{q}}\right]$$
$$-\left[\frac{A^{(2)}}{4\beta_1^2}-\frac{A^{(1)}}{4\beta_1}\ln\left[\frac{1}{2}e^{2\gamma-1}\right]\right]\ln\left[\frac{\hat{q}}{-\hat{b}}\right]-\frac{A^{(1)}\beta_2}{32\beta_1^3}[\ln^2(2\hat{q})-\ln^2(-2\hat{b})]\ . \tag{14}$$

The coefficients $A^{(i)}$ and β_i are

$$A^{(1)}=\frac{4}{3},\quad A^{(2)}=\frac{67}{9}-\frac{\pi^2}{3}-\frac{10}{27}n_f+\frac{8}{3}\beta_1\ln\left[\frac{1}{2}e^{\gamma}\right],$$
$$\beta_1=\frac{33-2n_f}{12},\quad \beta_2=\frac{153-19n_f}{24}\ , \tag{15}$$

where n_f, which takes the value 3 here, is the quark flavor number and γ is the Euler constant. Note that the lower bounds of $\bar{\mu}$ are arranged in a symmetric way in Eq. (13) so that the exponential suppression, which still obeys the renormalization-group equation of the wave function, is independent of the sequence of $\mathbf{b}_i$ in $\mathcal{P}$. The dimensional constant f_N, associated with the wave function ϕ, has the same evolution parameter w.

The renormalization group analysis of H gives

$$H_j(x_i,x_i',\mathbf{b}_i,Q,\mu)=\exp\left[3\sum_{l=1}^{2}\int_{t_{jl}}^{\mu}\frac{d\bar{\mu}}{\bar{\mu}}\gamma_q[g(\bar{\mu}^2)]\right]$$
$$\times H_j(x_i,x_i',\mathbf{b}_i,Q,t_{j1},t_{j2})\ . \tag{16}$$

Similar to Eq. (13), two lower bounds are inserted for $\bar{\mu}$. We adopt this form in order to assign to each hard gluon its individual largest mass scale as the argument of the corresponding α_s. The explicit expressions for t's are

$$t_{11}=\max[\sqrt{(1-x_1)(1-x_1')}Q,1/\tilde{b}_1]\ ,$$
$$t_{21}=\max(\sqrt{x_1x_1'}Q,1/\tilde{b}_1)\ , \qquad (17)$$
$$t_{12}=t_{22}=\max(\sqrt{x_2x_2'}Q,1/\tilde{b}_2)\ .$$

A detailed discussion about this arrangement will be given in Appendix C. The running coupling constant may be still large when the gluon energy and $1/\tilde{b}$ are both small. However, this nonperturbative region is Sudakov suppressed by the wave functions in Eq. (13) and is not important.

Inserting Eqs. (13) and (16) into Eq. (12), we have

$$F_1^p(Q^2)=\sum_{j=1}^{2}\frac{4\pi}{27}\int_0^1(dx)(dx')\int_0^\infty\tilde{b}_1d\tilde{b}_1\tilde{b}_2d\tilde{b}_2\int_0^{2\pi}d\theta[f_N(w)]^2H_j(x_i,x_i',\tilde{b}_i,Q,t_{j1},t_{j2})\Psi_j(x_i,x_i',w)$$
$$\times\exp[-S(x_i,x_i',\tilde{b}_i,Q,t_{j1},t_{j2})]\ , \qquad (18)$$

where

$$H_1=\tfrac{2}{3}\alpha_s(t_{11}^2)\alpha_s(t_{12}^2)K_0[\sqrt{(1-x_1)(1-x_1')}Q\tilde{b}_1]K_0(\sqrt{x_2x_2'}Q\tilde{b}_2)\ ,$$
$$H_2=\tfrac{2}{3}\alpha_s(t_{21}^2)\alpha_s(t_{22}^2)K_0(\sqrt{x_1x_1'}Q\tilde{b}_1)K_0(\sqrt{x_2x_2'}Q\tilde{b}_2)$$

are derived from the Fourier transform of Eq. (10). In Eq. (18), θ is the angle between $\mathbf{b}_1$ and $\mathbf{b}_2$, whose dependence resides in $\tilde{b}_3$. K_0 is the modified Bessel function of order zero. The expression for Ψ_j is the same as that in Eq. (11) but with $\psi(k_i,P,\mu)$ replaced by $\phi(x_i,w)$. The exponent S of complete Sudakov suppression is given by

$$S=\sum_{l=1}^{3}\left[s(x_l,\tilde{b}_l,Q)-\int_{1/\tilde{b}_l}^{t_{j1}}\frac{d\bar{\mu}}{\bar{\mu}}\gamma_q[g(\bar{\mu}^2)]\right]$$
$$+\sum_{l=1}^{3}\left[s(x_l',\tilde{b}_l,Q)-\int_{1/\tilde{b}_l}^{t_{j2}}\frac{d\bar{\mu}}{\bar{\mu}}\gamma_q[g(\bar{\mu}^2)]\right]\ . \qquad (19)$$

For the wave function, we will primarily consider the CZ model. Another proton wave function, the KS model [12], is also studied in order to test the sensitivity of our perturbative expression to the choice of different wave functions. Both the CZ and KS models are decomposed in terms of the first six Appel polynomials $A_j(x_i)$, which are eigensolutions of the evolution equation for the nucleon wave function [2,4]

$$\phi(x_i,w)=\phi_{as}(x_i)\sum_{j=0}^{5}N_j\left[\frac{\alpha_s(w^2)}{\alpha_s(\mu_0^2)}\right]^{b_j/\beta}a_jA_j(x_i)\ , \qquad (20)$$

where $\mu_0\approx1$ GeV. The constants N_j, a_j, and b_j are given in Table II. $\phi_{as}(x_i)=120x_1x_2x_3$ is the asymptotic form of ϕ. The evolution of the dimensional constant f_N is given by

$$f_N(w)=f_N(\mu_0)\left[\frac{\alpha_s(w^2)}{\alpha_s(\mu_0^2)}\right]^{2/(3\beta)}\ , \qquad (21)$$

where

$$f_N(\mu_0)=(5.2\pm0.3)\times10^{-3}\ \text{GeV}^2$$

(Ref. [7]) and $\beta=11-2n_f/3=9$ for $n_f=3$.

Before proceeding into numerical evaluation we examine the convergence of the integral in Eq. (18). It is apparent that ϕ and f_N, due to evolution, increase without limit as $w\to1/\Lambda$. In fact, the coefficients of the Appel polynomials become so large near this end that the series expansion of ϕ loses its accuracy. However, this region is suppressed by the Sudakov factors again. At the same time, the end-point singularities contained in Ψ and modified Bessel functions are also removed by $\phi_{as}(x_i)$ and $\phi_{as}(x_i')$. Therefore, the integral is well defined.

IV. NUMERICAL RESULTS

The typical behavior of Sudakov suppression on the line $\tilde{b}_1=\tilde{b}_2=b$ is shown in Fig. 4. Note that we have set the Sudakov exponential $\exp(-S)$ to unity in the small b region where it includes a small enhancement, since in this region it should be considered as the higher-order corrections to the hard scattering [1]. Therefore, we have also set any factor $e^{-s(\xi,\tilde{b},Q)}$ to unity whenever $\xi<\sqrt{2}/(Q\tilde{b})$. Then, $\exp(-S)$ decreases and vanishes as

TABLE II. Appel polynomial coefficients in Eq. (20) for the nucleon wave function $\phi(x_i,w)$ of the CZ and KS models [7,12] with the scale $\mu_0\approx1$ GeV [8].

j	a_j (CZ)	a_j (KS)	N_j	b_j	$A_j(x_i)$
0	1.00	1.00	1	0	1
1	0.410	0.310	$\frac{21}{2}$	$\frac{20}{9}$	x_1-x_3
2	−0.550	−0.370	$\frac{7}{2}$	$\frac{24}{9}$	$2-3(x_1+x_3)$
3	0.357	0.630	$\frac{63}{10}$	$\frac{32}{9}$	$2-7(x_1+x_3)+8(x_1^2+x_3^2)+4x_1x_3$
4	−0.012 2	0.003 33	$\frac{567}{2}$	$\frac{40}{9}$	$x_1-x_3-(4/3)(x_1^2-x_3^2)$
5	0.001 06	0.063 2	$\frac{81}{5}$	$\frac{42}{9}$	$2-7(x_1+x_3)+14x_1x_3$ $+\frac{14}{3}(x_1^2+x_3^2)$

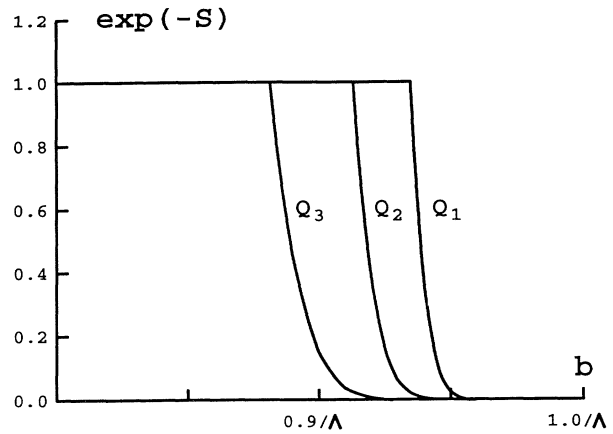

FIG. 4. Behavior of Sudakov suppression on the line $\tilde{b}_1=\tilde{b}_2=b$ for energy $Q_1/\Lambda=20$, $Q_2/\Lambda=30$, and $Q_3/\Lambda=50$ with $x_1=x_3=0.3$, $x_2=0.4$, $x_1'=x_3'=0.3$, $x_2'=0.4$, and $\theta=0.0$.

$b\rightarrow 1/\Lambda$. The variable b, like the loop momentum, can be integrated from 0 to ∞ in PQCD. The cutoff $1/\Lambda$, though larger than the nucleon size $\sim 1/(300\ \text{MeV})$, is set by the perturbative Sudakov factors. The large-b region is suppressed as expected and the suppression becomes stronger for larger Q. Note the scales on b axis. Sudakov suppression in the proton form factor is more moderate compared to that in the case of pion. This is because the former contains more γ_q's whose contributions give enhancement.

In order to investigate whether the perturbative region dominates, we analyze how the contributions to $Q^4F_1^p(Q^2)$ are distributed in $\tilde{b}_1$-$\tilde{b}_2$ plane. The integration is done with both variables $\tilde{b}_1$ and $\tilde{b}_2$ cut off at value b_c. If the perturbative region dominates, most of the contributions will be quickly accumulated below a small b_c. The numerical outcomes are shown in Fig. 5 with an approximate error ± 0.02 GeV^4, where Λ is set to 0.1 GeV. All the curves, showing the dependence of $Q^4F_1^p(Q^2)$ on b_c, increase from the origin and reach their full height at $b_c=1/\Lambda$, beyond which any remaining contributions are considered as totally nonperturbative. Note the particular behavior of the curve denoted by $Q_1/\Lambda=20$, which peaks at $b_c=0.8/\Lambda$ and then falls from 1.1 to 0.4 GeV^4 dramatically. It indicates that the nonperturbative region gives a large negative contribution due to evolution of the wave function, and that the self-consistency of calculation at this energy scale is questionable. For $Q_2/\Lambda=30$, the fierce variation of wave functions near the high end of b_c has been moderated by Sudakov suppression, as shown by the small hump of the corresponding curve. At the still higher energy, $Q_3/\Lambda=50$, the contribution from the large $\tilde{b}_1$-$\tilde{b}_2$ region is substantially zero. It implies that more and more contributions move into the perturbative region as Q increases.

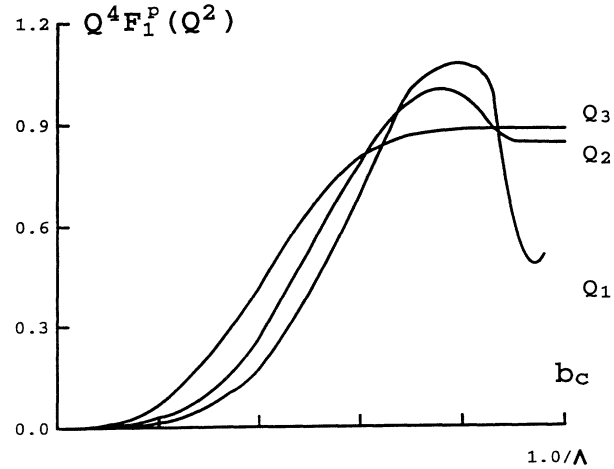

FIG. 5. Dependence of $Q^4F_1^p(Q^2)$ on the cutoff b_c with the CZ wave function. The energies Q_1, Q_2, and Q_3 are as in Fig. 4.

TABLE III. The values of $b_{1/2}$ for different energies. The magnitudes of α_s^2 with the argument evaluated at $1/b_{1/2}^2$ are also listed for reference.

Q/Λ	$b_{1/2}\Lambda$	$\alpha_s^2(1/b_{1/2}^2)$
30	0.46	0.81
40	0.44	0.72
50	0.42	0.65

A quantitative measure of self-consistency is the Q dependence of the cutoff $b_{1/2}$, up to which 50% of the whole amount of $Q^4F_1^p(Q^2)$ has been accumulated. The values of $b_{1/2}$ for different energies Q are listed in Table III. If 50% comes from the region where α_s^2 is smaller than 1, for example, $0.8[(\alpha_s/\pi)^2\sim 0.1]$, we have confidence that the calculation is at least minimally self-consistent. Based on this optimistic standard, even the results with $Q>3$ GeV are reliable. Therefore, the applicability of PQCD to the proton form factor at currently accessible energy scale $Q\sim 6$ GeV is justified.

In Fig. 6, we compare our predictions for $Q^4F_1^p(Q^2)$ to

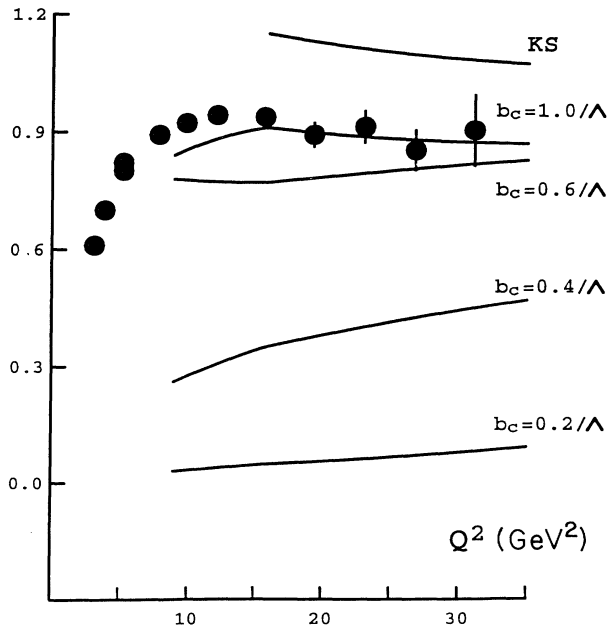

FIG. 6. Dependence of $Q^4F_1^p(Q^2)$ on the momentum transfer Q^2 for $\Lambda=0.1$ GeV with different b_c. The results from the KS wave function are also shown for $b_c=1/\Lambda$.

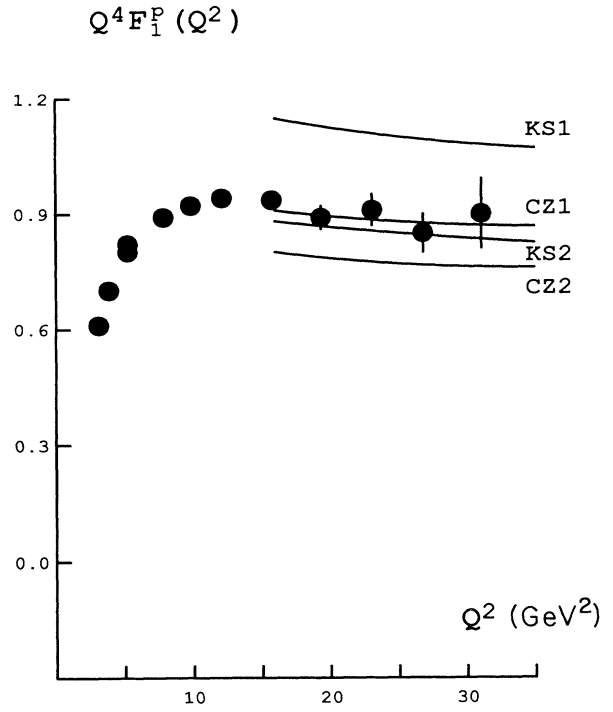

FIG. 7. Dependence of $Q^4F_1^p(Q^2)$ on the momentum transfer Q^2. CZ1 (CZ2) denotes the curve corresponding to $\Lambda=0.1$ (0.2) GeV for the use of the CZ wave function. KS1 and KS2 are defined similarly for the KS wave function.

experimental results, which are extracted from the data of elastic electron-proton cross section [8,18]. The increase of our predictions with the cutoff b_c is shown by a set of curves. The match between the curve for which $b_c=1/\Lambda$ and the data is obvious, not only in magnitude but also in the trend of variation on Q^2, arising at lower momentum transfers and then decreasing slowly with logarithmic dependence. For $Q<3$ GeV, the agreement is not quite as good. We observe that, from Fig. 5 and 6, the transition to PQCD as Q^2 increases is somewhat slower for the proton form factor than for the pion one. This is because the hard gluon exchange diagrams in the former case give leading contributions of order $(\alpha_s/\pi)^2$, rather than α_s/π, so that soft contributions, always suppressed by a power of M^2/Q^2 with M a typical hadronic mass, become relatively stronger [17].

Figure 6 also shows that the use of the KS model generates values which are larger than those from the CZ model only by a factor of about 20%. Referred to the results derived from the leading-order leading-power formula in Ref. [8], our expression is less sensitive to the choice of different wave functions. The third model, the Gari-Stefanis wave function, is also inserted into Eq. (18) and produces a similar curve located between the CZ and KS ones. We do not exhibit it for simplicity.

The sensitivity of our predictions to the variation of the QCD scale parameter Λ is easily examined. We find that the increase of Λ to 0.2 GeV enlarges $b_{1/2}$ and reduces $Q^4F_1^p$ by factors of about 10% when $Q\sim5$ GeV. The results derived from the KS wave function are then close to the data as shown in Fig. 7, where the values of $Q^4F_1^p$ for $\Lambda=0.1$ and 0.2 GeV obtained from the CZ and KS wave functions are displayed. Therefore, the data are still located in the range of our predictions.

V. CONCLUSION

The motivation for this work comes from the observation that the approach of the standard leading-order leading-power descriptions [2,19,21] to perturbative behavior is relatively slow and they are not reliable even at the highest available energies [6]. We have been able to explain self-consistently the experimental data of the proton Dirac form factor for $Q>3$ GeV. The essential feature of our perturbative calculation is the inclusion of Sudakov effects, from which the distribution amplitude is found to be suppressed in the large-b region. With the help of Sudakov suppression, the divergences in the running coupling constant, and in the evolution of the wave function are controlled and PQCD enlarges its range of applicability down to accessible energy scales. We should emphasize that QCD results must contain both perturbative and non-perturbative parts. Therefore, we do not propose a fully perturbative expression in this paper but the one in which the nonperturbative region denoted by $b\rightarrow1/\Lambda$ does become less important. Clearly, α_s is not so small that we should consider the perturbative result as exact, but it is sensible to compare it to experiment and to consider agreement as a success of the theory.

The suppression of hadron wave functions at large spatial extent is also crucial to the idea of "color transparency" [25] in the PQCD treatment of scattering processes involving nuclei. Our approach provides a careful check on the validity of the idea. If it is found, by a similar analysis, that main contribution comes from the region of sufficiently small b, for example, compared to the radius of a nucleus, hadronic systems can be thought of as carrying small color dipole moments, and thus interact weakly with the nuclear matter they pass through.

It is worth reemphasizing that our predictions, valid to $O(\alpha_s^2)$, can fit the experimental data without introducing an adjustable parameter into the calculation and are relatively insensitive to different models of wave functions. The cutoff preventing α_s from being singular is implemented by taking into account the transverse momenta, instead of inserting a gluon or quark mass [8,24]. From this point of view, our expression is more predictive. However, our approach still has to be complemented by the other derivations of the form factors, for instance those based on QCD sum rules [26] at moderate energies, where the perturbative contributions have not dominated.

ACKNOWLEDGMENTS

I thank Professor G. Sterman for helpful discussions and careful corrections. This work was supported in part by the National Science Foundation under Grant No. NSF-9211367, and by the National Science Council of the Republic of China under Grant No. NSC82-0112-C001-017.

APPENDIX A

In this Appendix, we present the explicit calculation of the integrand

$$\bar{Y}_{\alpha'\beta'\gamma'}H_{\alpha'\beta'\gamma'\alpha\beta\gamma}Y_{\alpha\beta\gamma}$$

for Fig. 2(a). Contributions from the other diagrams can be obtained by similar procedures.

In terms of the functions ψ and T, the distribution amplitude $Y_{\alpha\beta\gamma}(k_i,P,\mu)$ in Eq. (4) is reexpressed as

$$Y_{\alpha\beta\gamma}=\frac{f_N}{16\sqrt{2}N_c}(\mathcal{M}^1_{\alpha\beta\gamma}\psi_{123}+\mathcal{M}^2_{\alpha\beta\gamma}\psi_{213}+2\mathcal{M}^3_{\alpha\beta\gamma}T_{123}) , \tag{A1}$$

where

$$\begin{aligned}\mathcal{M}^1_{\alpha\beta\gamma}&=(\not{P}C)_{\alpha\beta}(\gamma_5 N)_\gamma-(\not{P}\gamma_5 C)_{\alpha\beta}N_\gamma ,\\ \mathcal{M}^2_{\alpha\beta\gamma}&=(\not{P}C)_{\alpha\beta}(\gamma_5 N)_\gamma+(\not{P}\gamma_5 C)_{\alpha\beta}N_\gamma ,\\ \mathcal{M}^3_{\alpha\beta\gamma}&=-(\sigma_{\mu\nu}P^\nu C)_{\alpha\beta}(\gamma^\mu\gamma_5 N)_\gamma .\end{aligned} \tag{A2}$$

From the properties of the Dirac matrices and charge conjugation

$$C^\dagger=C^{-1}=-C ,$$

it is easy to derive the distribution amplitude $\bar{Y}$ for the final state,

$$\begin{aligned}\bar{Y}_{\alpha\beta\gamma}&\equiv\gamma^0_{\alpha\alpha'}\gamma^0_{\beta\beta'}\gamma^0_{\gamma\gamma'}Y^\dagger_{\alpha'\beta'\gamma'}\\ &=\frac{f_N}{16\sqrt{2}N_c}(\bar{\mathcal{M}}^1_{\alpha\beta\gamma}\psi_{123}+\bar{\mathcal{M}}^2_{\alpha\beta\gamma}\psi_{213}+2\bar{\mathcal{M}}^3_{\alpha\beta\gamma}T_{123}) ,\end{aligned} \tag{A3}$$

where

$$\begin{aligned}\bar{\mathcal{M}}^1_{\alpha\beta\gamma}&=(C^{-1}\not{P})_{\alpha\beta}(\bar{N}\gamma_5)_\gamma-(C^{-1}\gamma_5\not{P})_{\alpha\beta}\bar{N}_\gamma ,\\ \bar{\mathcal{M}}^2_{\alpha\beta\gamma}&=(C^{-1}\not{P})_{\alpha\beta}(\bar{N}\gamma_5)_\gamma+(C^{-1}\gamma_5\not{P})_{\alpha\beta}\bar{N}_\gamma ,\\ \bar{\mathcal{M}}^3_{\alpha\beta\gamma}&=-(C^{-1}\sigma_{\nu\mu}P^\nu)_{\alpha\beta}(\bar{N}\gamma_5\gamma^\mu)_\gamma .\end{aligned} \tag{A4}$$

Note that $\mathcal{M}^{1\dagger}_{\alpha\beta\gamma}$ in $Y^\dagger_{\alpha\beta\gamma}$ is defined as

$$\mathcal{M}^{1\dagger}_{\alpha\beta\gamma}=(\not{P}C)^\dagger_{\alpha\beta}(\gamma_5 N)^\dagger_\gamma-(\not{P}\gamma_5 C)^\dagger_{\alpha\beta}N^\dagger_\gamma .$$

The hard-scattering amplitude $H^{(a)}$ for Fig. 2(a) is given by

$$H^{(a)}_{\alpha'\beta'\gamma'\alpha\beta\gamma}(k_i,k_i',P,P')=\mathcal{C}e_u g^4\frac{(\gamma_p)_{\gamma'\gamma}[\gamma^\rho(\not{P}'-\not{k}_1'-\not{k}_3)\gamma_\lambda]_{\beta'\beta}[\gamma^\lambda(\not{P}'-\not{P}+\not{k}_1)\gamma^\mu]_{\alpha'\alpha}}{(P'-k_1'-k_3)^2(P'-P+k_1)^2(P-k_1-P'+k_1')^2(k_3-k_3')^2} , \tag{A5}$$

where the color factor $\mathcal{C}$ is evaluated to be

$$\mathcal{C}=\epsilon_{a'b'c'}(T^j)_{c'c}(T^jT^i)_{b'b}(T^i)_{a'a}\epsilon_{abc}=\tfrac{8}{3} \tag{A6}$$

for the color number $N_c=3$. T^i is related to the Gell-Mann matrices by $T^i=\lambda^i/2$. In fact, all the hard-scattering subdiagrams have the same color factor.

There are nine terms in the expansion of the integrand $\bar{Y}H^{(a)}Y$. The first term is, using the same techniques of deriving $\bar{Y}$ from Y, written as

$$\text{term } 1=\frac{f_N^2\psi_{123}\psi'_{123}}{4608}\bar{\mathcal{M}}^{1*}_{\alpha'\beta'\gamma'}H^{(a)}_{\alpha'\beta'\gamma'\alpha\beta\gamma}\mathcal{M}^1_{\alpha\beta\gamma}=\frac{e_u g^4 f_N^2\psi_{123}\psi'_{123}}{864}\frac{\mathcal{N}^{(a)}}{\mathcal{D}^{(a)}} , \tag{A7}$$

where

$$\begin{aligned}\mathcal{N}^{(a)}&=\mathrm{Tr}[\gamma^\rho(\not{P}'-\not{k}_1'-\not{k}_3)\gamma_\lambda\not{P}\gamma^\mu(\not{P}'-\not{P}+\not{k}_1)\gamma^\lambda\not{P}']\bar{N}(P')\gamma_\rho N(P)\\ &\quad+\mathrm{Tr}[\gamma^\rho(\not{P}'-\not{k}_1'-\not{k}_3)\gamma_\lambda\gamma_5\not{P}\gamma^\mu(\not{P}'-\not{P}+\not{k}_1)\gamma^\lambda\not{P}']\bar{N}(P')\gamma_5\gamma_\rho N(P) ,\\ \mathcal{D}^{(a)}&=[(1-x_1)Q^2+\mathbf{k}^2_{T_1}][x_3(1-x_1')Q^2+(\mathbf{k}_{T_3}-\mathbf{k}'_{T_1})^2]\\ &\quad\times[(1-x_1)(1-x_1')Q^2+(\mathbf{k}_{T_1}-\mathbf{k}'_{T_1})^2][x_3x_3'Q^2+(\mathbf{k}_{T_3}-\mathbf{k}'_{T_3})^2] .\end{aligned} \tag{A8}$$

In order to simplify the calculation, some approximation has to be made. It is observed that the fermion propagators are only linearly, instead of quadratically, divergent in x. Therefore, the transverse momenta associated with the virtual quarks are expected to be less important than those with the gluons, and are neglected. In this approximation, the traces of the Dirac matrices in $\mathcal{N}^{(a)}$ can be easily carried out. We have

$$\text{term } 1=\frac{e_u g^4}{54}\frac{f_N^2\psi_{123}\psi'_{123}P'P}{(1-x_1)(1-x_1')Q^4}\frac{[P'P\bar{N}(P')\gamma^\mu N(P)+i\epsilon^{\rho\nu\sigma\mu}P'_\nu P_\sigma\bar{N}(P')\gamma_5\gamma_\rho N(P)]}{[(1-x_1)(1-x_1')Q^2+(\mathbf{k}_{T_1}-\mathbf{k}'_{T_1})^2][x_3x_3'Q^2+(\mathbf{k}_{T_3}-\mathbf{k}'_{T_3})^2]} . \tag{A9}$$

Applying the explicit expressions for P, P', $\bar{N}(P')$, and $N(P)$, it can be shown that the two spinor products in Eq. (A9) have the same form.

The other terms can be derived similarly and their summation gives the complete expression

$$\bar{Y}_{\alpha'\beta'\gamma'}H^{(a)}_{\alpha'\beta'\gamma'\alpha\beta\gamma}Y_{\alpha\beta\gamma}=\bar{N}(P')\gamma^\mu N(P)I^{(a)} , \tag{A10}$$

where

$$I^{(a)}=\frac{4\pi^2/27e_u\alpha_s^2 f_N^2(\psi_{123}\psi'_{123}+4T_{123}T'_{123})}{(1-x_1)(1-x'_1)[(1-x_1)(1-x'_1)Q^2+(\mathbf{k}_{T_1}-\mathbf{k}'_{T_1})^2][x_3x'_3Q^2+(\mathbf{k}_{T_3}-\mathbf{k}'_{T_3})^2]} .$$

The coefficient of the electromagnetic vertex $\bar{N}\gamma^\mu N$, $I^{(a)}$, will be integrated to calculate $F_1^p(Q^2)$. Therefore, we list it in Table I.

APPENDIX B

In the derivation of the integrand $\bar{Y}HY$ for the diagrams in Fig. 2, the transverse momenta carried by the virtual quarks have been neglected. This approximation is necessary because the exact manipulation involves a high-dimensional integral which is almost impossible to compute. However, we have to examine the accuracy of the approximation to ascertain that our predictions are still reliable. We investigate a simpler case, the pion electromagnetic form factor, from which some rough estimations can be acquired about the errors associated with the results obtained in this paper.

The parallel formula to Eq. (18) for the pion form factor $F_\pi(Q^2)$ has been derived in Ref. [1]. We just quote the result here:

$$F_\pi(Q^2)=16\pi\mathcal{C}_F\int_0^1 dx_1dx_2\phi(x_1)\phi(x_2)\times\int_0^\infty b\,db\,\alpha_s(t)K_0(\sqrt{x_1x_2}Qb)\times\exp[-S(x_1,x_2,b,Q)] , \tag{B1}$$

where

$$S=\sum_{l=1}^{2}[s(x_l,b,Q)+s(1-x_l,b,Q)]-\frac{2}{\beta_1}\ln\left[\frac{\ln(t/\Lambda)}{-\ln(b\Lambda)}\right] ,$$

$$t=\max[\sqrt{x_1x_2}Q,1/b] .$$

It is straightforward to obtain its exact form from the complete expression of the hard-scattering kernel. We have

$$F_\pi(Q^2)=16\pi\mathcal{C}_F\int_0^1 dx_1dx_2\phi(x_1)\phi(x_2)\int_0^\infty b_1db_1b_2db_2\alpha_s(t)K_0(\sqrt{x_1x_2}Qb_1)\exp[-S(x_1,x_2,b_1,b_2,Q)]\times[\theta(b_1-b_2)K_0(\sqrt{x_1}Qb_1)I_0(\sqrt{x_1}Qb_2)+\theta(b_2-b_1)K_0(\sqrt{x_1}Qb_2)I_0(\sqrt{x_1}Qb_1)] , \tag{B2}$$

where

$$S=\sum_{l=1}^{2}[s(x_l,b_l,Q)+s(1-x_l,b_l,Q)]-\frac{1}{\beta_1}\ln\left[\frac{\ln(t/\Lambda)}{-\ln(b_1\Lambda)}+\frac{\ln(t/\Lambda)}{-\ln(b_2\Lambda)}\right] ,$$

$$t=\max[\sqrt{x_1x_2}Q^2,1/b_1,1/b_2] .$$

Both integrals in Eqs. (B1) and (B2) can be done numerically and the results are listed in Table IV for comparison. We find that the values for $Q^2F_\pi(Q^2)$ derived from the exact formula Eq. (B2) are smaller than those from the approximate one Eq. (B1), because reinstatement of transverse momentum into the quark propagator will reduce the integrand. At the same time, the correction becomes less apparent as Q increases. The errors are only 10% for $Q>3$ GeV. We estimate that the errors in the proton case are roughly of the same magnitude. Hence, the approximation does not weaken our conclusions.

TABLE IV. The values of $Q^2F_\pi(Q^2)$ derived from the formulas with and without approximation for the use of the CZ wave function [7] $\phi^{CZ}(x)=(15f_\pi/\sqrt{2N_c})x(1-x)(1-2x)^2$.

Energy Q/Λ	$Q^2F_\pi(Q^2)$ Approx	Exact	Err
10	0.27	0.20	26%
20	0.27	0.23	15%
30	0.26	0.23	11%
50	0.25	0.23	8%

APPENDIX C

In Eq. (16) we assign different arguments to α_s's corresponding to the two exchanged gluons in the hard scattering H instead of applying renormalization-group analysis to it as a whole. In this appendix we give more detailed explanation to support the legitimacy of Eq. (16) and investigate the sensitivity of our results to different choices of the arguments.

We separate the hard-scattering subdiagram into two parts as shown in Fig. 8, each box containing a single exchanged gluon. Then H is written as

$$H=\Gamma^l G\Gamma^r , \tag{C1}$$

where Γ^l (Γ^r) is the amplitude with four external quarks corresponding to the left-hand (right-hand) box, and the amplitude G is associated with the virtual quark line.

The renormalization-group equation for H leads to

$$\frac{\mathcal{D}(\Gamma^l G^{1/2})}{\Gamma^l G^{1/2}}+\frac{\mathcal{D}(\Gamma^r G^{1/2})}{\Gamma^r G^{1/2}}=6\gamma_q \ , \tag{C2}$$

where

$$\mathcal{D}\equiv\mu\frac{\partial}{\partial\mu}+\beta(g)\frac{\partial}{\partial g} \ . \tag{C3}$$

Equation (16) is obtained if we use the individual renormalization-group equations for the boxed diagrams of Fig. 8:

$$\begin{aligned}\mathcal{D}(\Gamma^l G^{1/2})&=3\gamma_q\Gamma^l G^{1/2} \ ,\\ \mathcal{D}(\Gamma^r G^{1/2})&=3\gamma_q\Gamma^r G^{1/2} \ .\end{aligned} \tag{C4}$$

Certainly the solution to Eq. (C4) does not sum up all the logarithms included in H due to radiative corrections. However, Eq. (C4) may be thought of as an approximation, and we can examine the sensitivity of the predictions to this approximation.

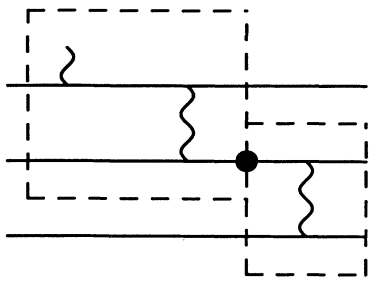

FIG. 8. One of the hard-scattering subdiagrams for the derivation of Eq. (16).

If the exact solution to Eq. (C2) is employed, a single t will be chosen for the arguments of α_s's, for example, as the maximum of the averages of scales

$$t_1=t_{11}=t_{12}=\max\left[\frac{1}{2}\left[\sqrt{(1-x_1)(1-x_1')}Q+\sqrt{x_2x_2'}Q\right],\frac{2}{\tilde{b}_1+\tilde{b}_2}\right] \ ,$$

$$t_2=t_{21}=t_{22}=\max\left[\frac{1}{2}\left[\sqrt{x_1x_1'}Q+\sqrt{x_2x_2'}Q\right],\frac{2}{\tilde{b}_1+\tilde{b}_2}\right] \ .$$

It is found that the results for $Q^4F_1^p(Q^2)$ based on this assignment are decreased only by a factor of 7%, which are still in agreement with the data. Therefore, our predictions are not sensitive to different choices of the arguments of α_s's. For the purpose of truly reflecting the individual virtuality of each hard gluon, Eq. (16) is thus an appropriate form.

[1] H. N. Li and G. Sterman, Nucl. Phys. **B381**, 129 (1992).

[2] G. P. Lepage and S. J. Brodsky, in *Quantum Chromodynamics (La Jolla Institute 1978)*, Proceedings of the Workshop, La Jolla, California, edited by W. Frazer and F. Henyey, AIP Conf. Proc. No. 55 (AIP, New York, 1979); presented at the Workshop on Current Topics in High Energy Physics, Pasadena, California, 1979 (unpublished); Phys. Rev. Lett. **43**, 545 (1979); Phys. Rev. D **22**, 2157 (1980).

[3] I. G. Aznauryan, S. V. Esaybegyan, and N. L. Ter-Isaakyan, Phys. Lett. **90B**, 151 (1980); **92B**, 371(E) (1980); A. Duncan and A. H. Mueller, Phys. Rev. D **21**, 1636 (1980).

[4] S. J. Brodsky and G. P. Lepage, Phys. Scr. **23**, 945 (1981).

[5] V. A. Avdeenko, V. L. Chernyak, and S. A. Korenbilt, Yad. Fiz. **33**, 481 (1981) [Sov. J. Nucl. Phys. **33**, 252 (1981)].

[6] N. Isgur and C. H. Llewellyn Smith, Phys. Rev. Lett. **52**, 1080 (1984); A. V. Radyushkin, Acta Phys. Polonica B **15**, 403 (1984); A. P. Bakulev and A. P. Radyushkin, Phys. Lett. B **271**, 223 (1991).

[7] V. L. Chernyak and A. R. Zhitnitsky, Yad. Fiz. **31**, 1053 (1980) [Sov. J. Nucl. Phys. **31**, 544 (1980)]; Nucl. Phys. **B216**, 373 (1983); **B246**, 52 (1984); Phys. Rep. **112**, 173 (1984).

[8] C. R. Ji, A. F. Sill, and R. M. Lombard-Nelsen, Phys. Rev. D **36**, 165 (1987).

[9] C. E. Carlson and F. Gross, Phys. Rev. D **36**, 2060 (1987).

[10] V. M. Belyaev and B. L. Ioffe, Zh. Eksp. Teor. Phys. **83**, 876 (1982) [Sov. Phys. JETP **56**, 493 (1982)].

[11] N. Isgur and C. H. Llewellyn Smith, Nucl. Phys. **B317**, 526 (1989).

[12] I. D. King and C. T. Sachrajda, Nucl. Phys. **B279**, 785 (1987).

[13] M. Gari and N. G. Stefanis, Phys. Lett. B **175**, 462 (1986).

[14] J. M. Cornwall, Phys. Rev. D **26**, 1453 (1982).

[15] J. Botts and G. Sterman, Nucl. Phys. **B325**, 62 (1989).

[16] J. C. Collins, in *Perturbative Quantum Chromodynamics*, edited by A. H. Mueller (World Scientific, Singapore, 1989).

[17] A. V. Radyushkin, Nucl. Phys. **A532**, 141 (1991).

[18] G. Arnold *et al.*, Phys. Rev. Lett. **57**, 174 (1986).

[19] G. R. Farrar and D. R. Jackson, Phys. Rev. Lett. **43**, 246 (1979).

[20] G. P. Lepage and S. J. Brodsky, Phys. Lett. **87B**, 359 (1979).

[21] A. V. Efremov and A. V. Radyushkin, Phys. Lett. **94B**, 245 (1980).

[22] S. J. Brodsky and G. R. Farrar, Phys. Rev. D **11**, 1309 (1975).

[23] B. L. Ioffe, Nucl. Phys. **B188**, 317 (1981); **B191**, 591(E) (1981).

[24] T. Huang and Q. X. Shen, Z. Phys. C **50**, 139 (1991).

[25] S. J. Brodsky and A. H. Mueller, Phys. Lett. B **206**, 685 (1988).

[26] V. A. Nesterenko and A. V. Radyushkin, Phys. Lett. **115B**, 410 (1982); B. L. Ioffe and A. V. Smilga, Nucl. Phys. **B216**, 373 (1983).